applied sciences

Review

Review of Control Technologies for Quiet Operations of Advanced Air-Mobility

Samuel Afari, Vladimir Golubev, Anastasios S. Lyrintzis and Reda Mankbadi *

Aerospace Engineering Department, Embry-Riddle Aeronautical University, Daytona Beach, FL 32114, USA
* Correspondence: reda.mankbadi@erau.edu (R.M.)

Abstract: The current technologies for developing quiet rotor noise in urban canyons are reviewed. Several passive noise control approaches are discussed with their limitations in reducing both tonal and broadband noise. Blade tip modifications are seen to be one of the more successful in reducing tonal noise, with serrations at the trailing edge useful in reducing trailing edge broadband noise. Due to the adverse performance limitations of passive control, several optimization approaches are reviewed to discuss the possible improvements in performance of rotors. Additionally, a few legacy control technologies for helicopters are discussed. Active control technologies are investigated. The overall outlook and challenges to these methods are discussed with an eye on Advanced Air Mobility Vehicles (AAM).

Keywords: active control; noise; AAMV; UAV; rotorcraft

check for updates

Citation: Afari, S.; Golubev, V.; Lyrintzis, A.S.; Mankbadi, R. Review of Control Technologies for Quiet Operations of Advanced Air-Mobility. *Appl. Sci.* **2023**, *13*, 2543. https://doi.org/10.3390/app13042543

Academic Editors: Junhong Park and Dan Zhao

Received: 27 November 2022
Revised: 28 December 2022
Accepted: 28 December 2022
Published: 16 February 2023

1. Introduction

The interest in Urban Advanced Air Mobility Vehicles (AAM), such as drones, electrical Vertical Take-off and Landing (eVTOL), and air taxis, has been significantly increasing. However, progress in its implementation is hindered by the concerns about its safety and the associated noise annoyance near vertiports [1–5]. From aerodynamic-point of view, the most safety-critical situations for civilian aircraft are during takeoff and landing. As such, the FAA has implemented specific flying procedures near airports to emphasize safety [1]. Realizing that aircraft noise is also a health-safety hazard to populations around airports, the FAA has modified the aircrafts takeoff and landing operations around airports to minimize the noise impact on the populations around airports, thus aero-safety and aero-noise are coupled.

AAM often encounter adverse environmental conditions near vertiport. This may include unsteady factors such as gust, concentrated vorticity, turbulence, and proximity to ground and other buildings. Wind variability produced by gusts could affect the eVTOL stability in takeoff and even in landing. In descent, vehicles lose their directivity and the aircraft's controllability may be significantly degraded. This, along with the vehicle unsteady maneuvering and rotor-rotor interactions, can lead to elevated noise. Edgewise-flying rotor noise, which is critical for descending flight into vertiports, needs to be studied. These elevated noise levels can impact go-no-go flight decisions and make recommendations for noise-mitigation techniques.

We review here passive and active control of AAM with an eye on operations near vertiport. We then discuss the outlook and challenges that need to be addressed. We discuss in Section 2, some passive control technologies as applied to reduction in both tonal and Broadband Noise (BBN). In Section 3 we discuss Multi-Disciplinary Optimization (MDO) as pertaining to balancing the noise reduction vs. performance. In Section 4 we review Active Noise Control (ANC) technologies. Discussions, outlook, and challenges are given in Section 5. It should be noted that this is not an exhaustive review, but rather a perspective to showcase some of the important noise reduction techniques for e-VTOL configurations.

2. Passive Control Technologies

Several ideas for passive control via design changes have been proposed to reduce the noise in various eVTOL configurations. The noise is usually classified as tonal and Broad-Band Noise (BBN). Tonal noise occurs at discrete frequencies, while BBN extends over a wide range of frequencies. The tonal noise is usually split into loading noise and thickness noise and is characterized by sharp tonal noise at the Blade-Passing-Frequency (BPF) and its harmonics. The BBN is created by turbulence effects and non-linearities in the flow [6] and originates from various sources, including, the turbulent leading or trailing edge of the boundary layer, and separation effects, among other sources. The discrete tones peak at harmonics of the Blade-Passing Frequency (BPF). In passive technology, usually the performance is adversely affected. Therefore, we need to balance noise levels with overall performance. Multi-Disciplinary Optimization (MDO) key to a successful design of such vehicles. Several ideas have been spurned to passively reduce the noise signatures of propellers over the past decade. We summarize here some of the passive technology proposed in AAM.

2.1. Tonal Noise Reduction

Historically, a great number of works have been undertaken to passively mitigate the acoustic signature of rotors and small-scale propellers of Unmanned Aerial Vehicles (UAV) and other AAM:

Ducting: Lu, et al. [7] researched the use of ducts with acoustic absorption materials to reduce the noise. They tested two ducts – one with perforated internal walls and one without perforations. Both ducts showed deleterious effects in thrust, with a 10–20% reduction in thrust, and overall noise level increase of ~5–10 dBA.

Stacking: Two propellers on top of each other was found to increase the overall propulsive efficiency [8,9]. Loss of thrust and propulsive efficiency was observed in the front (or top) propeller [9], while an increase in thrust and propulsive efficiency was observed for the bottom propeller. Diaz et al. [10] investigated the effects of ducts on coaxial rotors in hover using high-fidelity CFD [10]. They performed some qualitative acoustic analysis on the various configurations evaluated and saw that placing the duct around the lower propeller of the coaxial system resulted in reduced acoustic signature (see Figure 1). Clearly, here we see that there are some acoustic benefits to ducting and may need critical placement for peak noise cancellation.

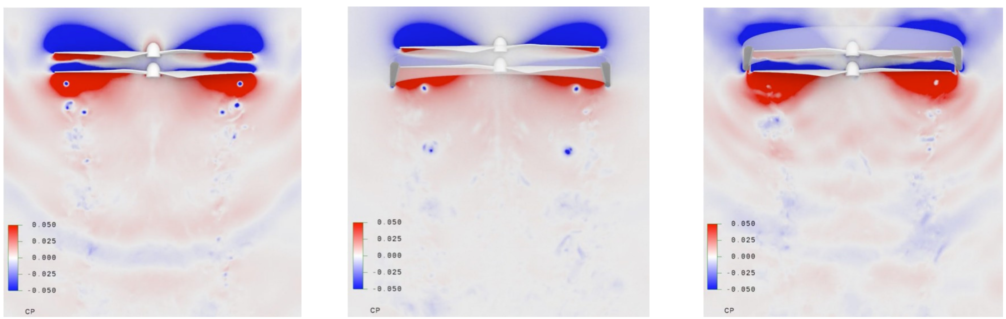

Figure 1. Pressure fluctuations for different configurations (counter-rotating). Left: open rotors, Center: duct around lower rotor, and Right: duct around upper rotor [10].

Blade Count and Spacing: For the same thrust, increasing the number of blades reduces the tonal noise. Increasing the number of blades from two blades to four blades resulted in 10 dB reduction, but also increases the frequency of the noise [11]. This may increase the broadband noise floor, and hence increase the perceived noise level. Unequal blade spacings were found to diminish tones at the BPF harmonics [11]. Reducing the diameter of the propeller reduces the tip Mach number for a given rotational rate and the noise as well.

A tip Mach number reduction from $M_T = 0.6$ to $M_T = 0.53$ was seen to have an acoustic energy difference of 6 dB [11].

Phase Control: Pascioni et al. [12] explored the potential of using Phase Control for noise reduction experimentally by utilizing a dual-rotor test stand. The two-bladed CF125 rotors were separated by a hub separation distance of 0.4 meters. Using a timing belt and mechanical adjustments, phasing and rotational rates are set for each of the blades. Noise measurements were performed using microphones installed in the Structural Acoustics Loads and Transmission (SALT) facility [13]. Using the experiments as validation, they developed a numerical model for further phasing studies of more configurations, varying the propeller count from 2 to 8 rotors. They showed that the overall directivity of the blade passage frequency noise can be modified, with a reduction as high as 28.6 dB recorded [12]. They also conclude that the deviation from the rotational rate between the two systems should not exceed 0.5% for a 6 dB blade passage frequency noise reduction.

Smith et al. [14] also found similar results numerically by varying the phase angles between the rotors and found quiet zones in the in-plane inter-boom bisections up to 20 dB. Similar work was done by Whiteside et al. [15] experimentally and numerically but focused more on stacked rotor performance. They utilized two sets of 3-bladed rotors, with at tip radius of 158.75 mm, and tested various axial and azimuthal offsets between the two rotors. They found that the configuration with the ratio of stack clearance distance to rotor radius ($\Delta Z/R$) = 0.15 to be the most efficient due to rotor power loading with a power savings of 6.9% relative to the coplanar case. The stacked rotor configurations showed increases in low frequency tonal noise with increasing axial separation and decreasing azimuthal offset. All the stacked rotor configurations showed broadband levels lower than that of the baseline rotor. An unweighted OASPL noise level reduction of 2.6 dB was measured below the plane of the lower rotor.

2.2. Broadband Noise Reduction

Serration and Trip Effects: Leslie, et al. [16] investigated the main sources of broadband noise for small scale propellers at low Reynolds numbers and found it to be mainly a result of the trailing edge boundary layer thickness caused by a laminar separation bubble on the suction side of the propeller. They used a leading-edge trip and serrations (Figure 2a,c) placed prior to the laminar separation to reduce trailing edge thickness which resulted in a decrease in turbulent boundary-layer trailing edge noise. They reported an overall broadband reduction of up to 4 dB in static tests at a rotational rate of 5000 rpm (see Figure 2b,d). Figure 2d shows that at the same operational conditions, the serrations had more broadband noise reduction at higher frequencies by about 2 dB. This may be a result of the effective magnitudes of the trailing edge noise sources, i.e., the trailing edge boundary layer interaction noise may be slightly more critical than the laminar separation bubble interaction noise. An important takeaway mentioned is that this method would only be effective for cases where there was a presence of a laminar separation bubble, which was mentioned to be the case only for cruise conditions, and thus would perform poorly for take-off conditions where blade loading is highest.

Cambray et al. [17] investigated the effects of trailing edge serrations on broadband noise reductions UAVs. They perform these tests on an experimental test rig with an 8-inch diameter 2-bladed propeller. They noted that an increase in pitch angles did increase the overall sound pressure levels both in the tonal and broadband noise levels of UAV propellers. Reduction in broadband noise levels were achieved using trailing edge serrations. The results suggested that the noise reduction is due to the interaction between the serrations and the trailing edge boundary layer, which is a dominant source of high-frequency broadband noise. The depth of the serration also has an effect in the amount of reduction in SPL that can be achieved with the larger depths resulting in higher BBN reduction of 3 dB at 3 kHz and increases to a 5 dB reduction at 10 kHz (see Figure 3d, where Case 3 is highest depth/amplitude of serration). Additionally, the effectiveness of this technique is reported to diminish with increasing rotational rates, and thus is only recommended at lower tip speed rotors/propellers. It is important here to note that although the targeted high-frequency broadband noise was reduced, there may be an increase in the tonal noise levels as seen in Figure 3d. As such, care must be taken in selecting the right serration wavelength/size.

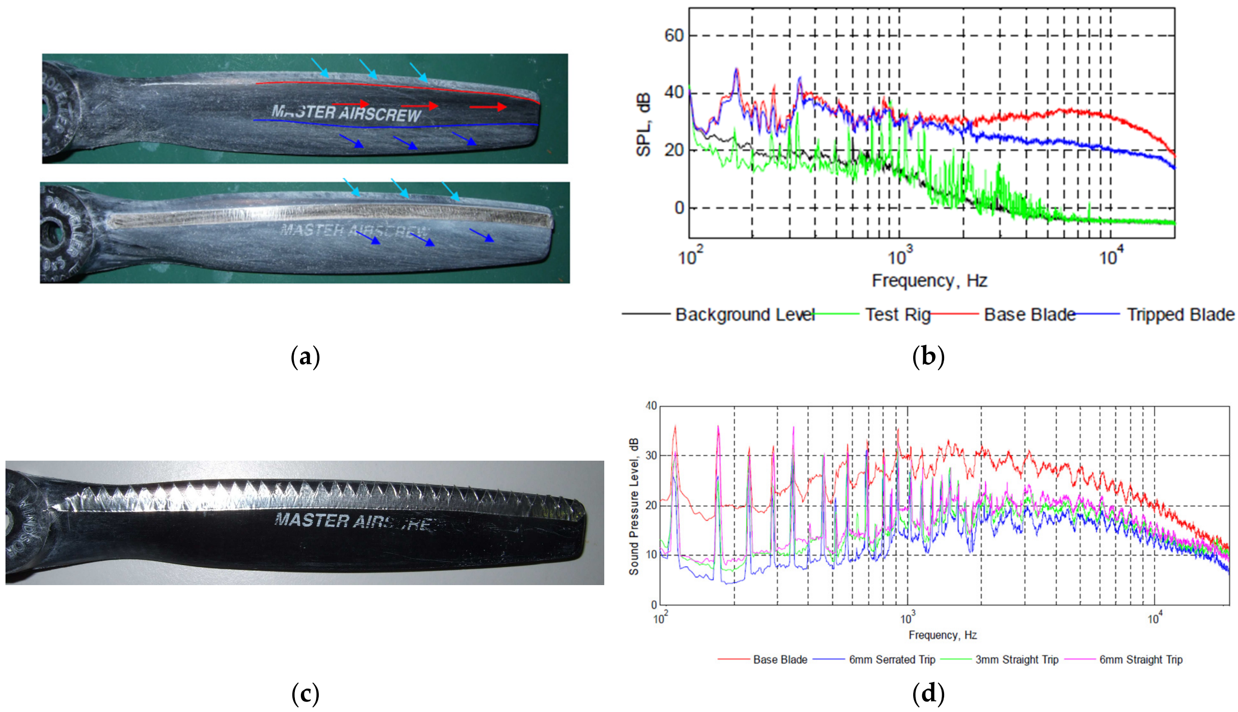

Figure 2. Effects of LE trip and serration as a passive noise control technique [16]. (**a**) Base propeller (top) and leading-edge tripped propeller (bottom). (**b**) Spectra showing effect of LE trip in Wind tunnel tests (V = 10 m/s, 5000 RPM). (**c**) Schematic of propeller showing Leading-edge serrations. (**d**) Spectra showing effects of various serration depths. Reprinted with permission from Wong, K.C. (2008).

Similar work was done by Intravartolo et al. [18], where they focused on the effect of the saw-toothed serration on the strength of the trailing wake, and subsequently the overall noise signature of the propeller. They reported an approximately linear reduction in SPL measurements for an increase in serration depth, with a 46.67% chord depth serration cut resulting in approximately 28% decrease in noise.

Another novel idea was proposed by Nelson [19] and implemented by Demoret and Wisniewski [20]. They utilized a DJI Phantom 2-bladed propeller with a diameter of 9.4 inches ad a pitch of 5 inches. The noise measurements are performed below the rotor and are traversed from hub to tip. They examined the effects of adding a leading-edge notch to the stock blade by cutting a grove in the blade (see Figure 4). They reported that placing the notch at r/R of 0.90 resulted in 25% (~30 dB) reduction in peak SPL at a detriment of 9% increase in power required for similar thrust conditions. The main idea behind the notch approach was to disrupt the tip vortices rolling off the blade tips which is one of the major sources of propeller aerodynamic noise. This approach has a potential for noise control but again, has a penalty of thrust and power increase. Additionally, this may lead to some structural limitations for scaling to larger rotors.

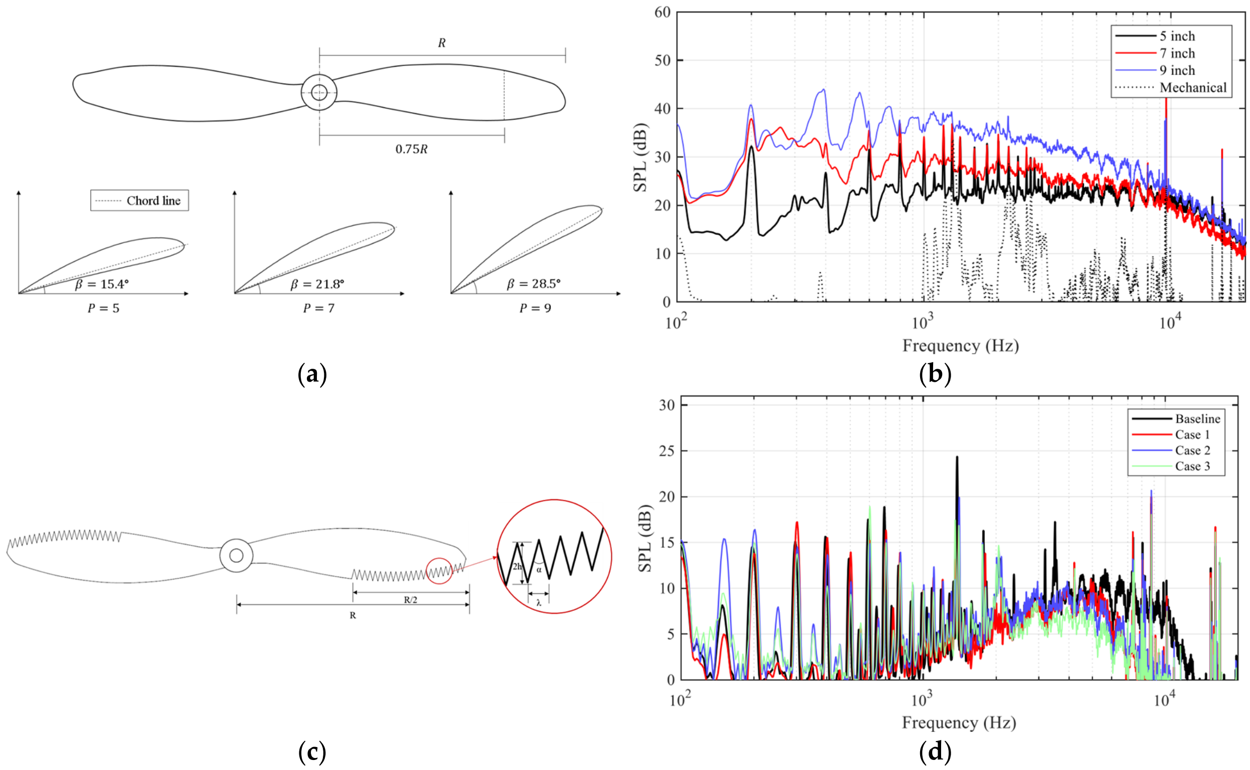

Figure 3. Effects of pitch angle and TE serrations as a passive noise control technique [17]. (**a**) Schematic of propeller with different pitch angles. (**b**) Spectra showing effects of pitch angles. (**c**) Schematic of propeller showing Trailing edge serrations. (**d**) Spectra showing effects of various serration depths and angles at 3000 rpm. Reprinted with permission from Azarpeyvand, M. (2018).

Figure 4. Schematic of Propeller configurations; stock blade (**left**) and notch or cut at leading edge of blade (**right**) [20].

A more thorough review of passive and some active control methods for helicopters is discussed by Schmitz [21]. In summary, a lot of work has been done to passively control the noise of propellers. One disadvantage of passive methods is that these methods, although arguably effective in reducing noise levels, do affect the performance of the blades. As such, it is beneficial to investigate actively controlling rotor noise, especially when needed, such as near vertiports/heliports, while maintaining performance, perhaps via optimization.

3. Multi-Disciplinary Optimization in Aeroacoustics

As pointed out earlier, Multi-Disciplinary Optimization (MDO) is needed to balance the noise reduction achieved via passive design changes to reduce noise vs the decrease in performance. Optimization consists of the use of algorithms to minimize or maximize a specific set of functions by varying several variables [22]. It is a technique generally used in design of complex systems hoping to maximize or reduce a specific measure of performance. The idea of MDO is to be able to not only perform the optimization based on the performance of individual disciplines, but also the interactive effects of multiple disciplines on a specific objective. One of the first aerodynamic shape optimization papers which proposed the use of adjoint methods for sensitivity analysis was Pironneau in 1975 [23]. One of the first multidisciplinary design optimization applications was performed on aircraft wing design, where aerodynamics, structures and controls were tightly coupled [24,25]. In more recent years, the application of MDO has been applied to the design of complete aircrafts [26,27], as well as a rotorcraft design [28,29].

Noise Reduction within Optimization Framework

Once again, a lot of research has been done with the focus of MDO for rotors and propellers with an acoustic constraint. Pagano et al. [30] discussed an optimization method of coupling unsteady aerodynamic and structural dynamic models to account for the aero-elastic effects of the propeller. They utilize the 6-bladed propeller of the Piaggio P.180 Avanti aircraft (see Figure 5, Planform view of single blade, from root to tip) with an angular velocity of 188.5 rad/s. The aerodynamic parameters of surface pressures were generated using a "full potential" CFD model with a turbulent boundary layer model based on the "defect formulation theory". This was loosely coupled with a computational structural dynamics code (CSD). The blade loads information, as well as the boundary layer parameters were then used as input for tonal and broadband noise predictions using the Ffowcs Williams Hawkings equations [31] for tonal content, and Amiet's equations [30] for turbulent boundary layer broadband noise. They applied this method to propellers in aircraft pusher configurations, with a performance constraint of shaft power availability of 633.8 kW for take-off condition, as well as an acoustic minimization constraint. Because much of the noise at such high rotational rates stems from the tip speeds, the optimal solution was obtained by modifying the tip geometries as seen in Figure 5. They realized an overall sound pressure level reduction of 3.5 dB at 45°, 20 m away from the propeller axis at the take-off condition with the optimized blade geometry.

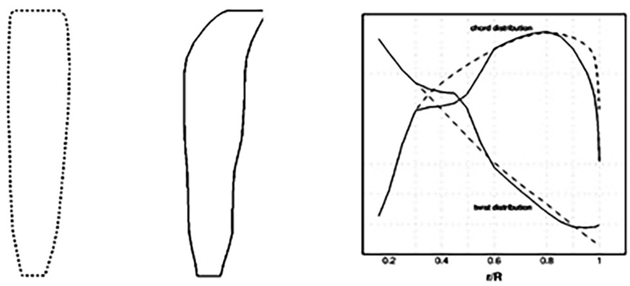

(a) Planforms view **(b) Twist and chord radial variation laws**

Figure 5. Comparison between reference blade (dashed line), and optimized blade (solid line) [31]. Reprinted with permission from Pagano, A. (2010).

Similar work was done by Marinus et al. [32] in which they utilized a Multi-Objective Differential Evolution (MODE) technique coupled with a genetic algorithm to optimize propeller blades for transonic flow. By allowing the algorithm to vary geometric variables such as airfoil chord, camber line, thickness ratio, and twist, generations of solutions were obtained. High-fidelity RANS simulations were performed and Ffowcs-Williams Hawkings equations [33] were utilized for noise computations at 4 Rotor radii away. A BPF noise reduction of 5.2 dB was obtained for "individual B" configuration (see Figure 6d), which was postulated to be a result of the aerodynamic loads shifting from the tips to the optimized hump inward of the blades.

Variable		Number of Control Points	Number of parameters	
Chord length	$b(r)/D$	7	7	
Thickness ratio	$t(r)/b(r)$	4	3	
Geometrical sweep	$Sw(r)$	4	4	(1)
Twist	$Tw(r)$	4	3	
Airfoil *I* thickness	t_A	6	5	(2)
Airfoil *I* camberline	y_A	4	1	
Airfoil *II* thickness	t_B	6	5	(3)
Airfoil *II* camberline	y_B	4	2	
Total			30	

(1) defined as the angle between the axis of the blade and the stacking-line
(2) from blade root to 35% radius
(3) from 45% radius to blade tip

(**a**)

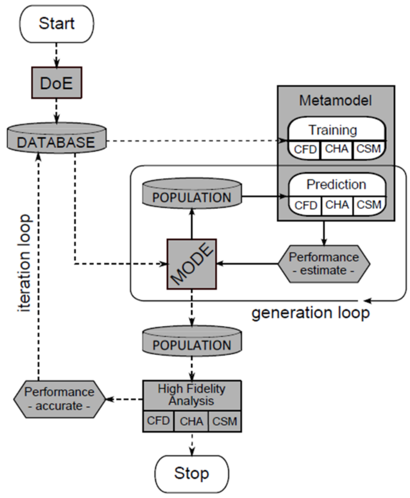

(**b**)

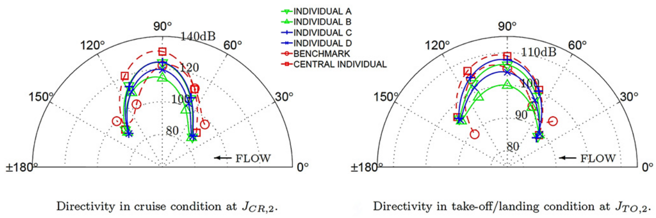

(**c**)

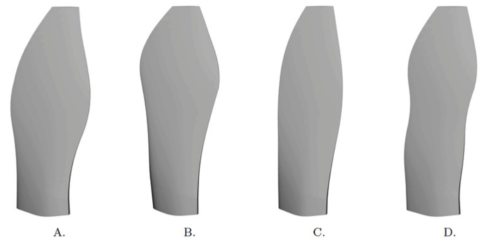

(**d**)

Figure 6. Optimization of blade geometry with acoustic constraint [32]. (**a**) Optimization Design Variables. (**b**) Workflow of Optimization Framework. (**c**) Noise Directivity of Optimized Blade Geometries. (**d**) Optimized Blade Geometries. Reprinted with permission from Marinus, B.G. (2011).

Jones et al. [34] designed an airfoil for low drag and low tonal noise using the genetic algorithm. They utilized an airfoil representative of a helicopter in forward flight, at three flight conditions summarized in Figure 7. The optimization constraints were to minimize form drag, and the acoustic signature in the form of OASPL at observer locations 50 m from the hub. They utilized XFOIL [35] for aerodynamics and WOPWOP [36] for aeroacoustics computations. The resulting optimized solution provided rather unconventional airfoil shapes that had about 25% improvement in the acoustic fitness function (OASPL) while maintaining a good aerodynamic performance compared to the NACA 0012 airfoil.

More recently Ingraham et al. [37] utilized a gradient-based propeller optimization with the focus on urban air mobility vehicle. Their work combined a blade element momentum theory tool "OpenBEMT" with an acoustic prediction tool "ANOPP2" within an optimization framework called OpenMDAO. They were able to achieve a 5dB reduction in OASPL at a cost of 1% propeller efficiency.

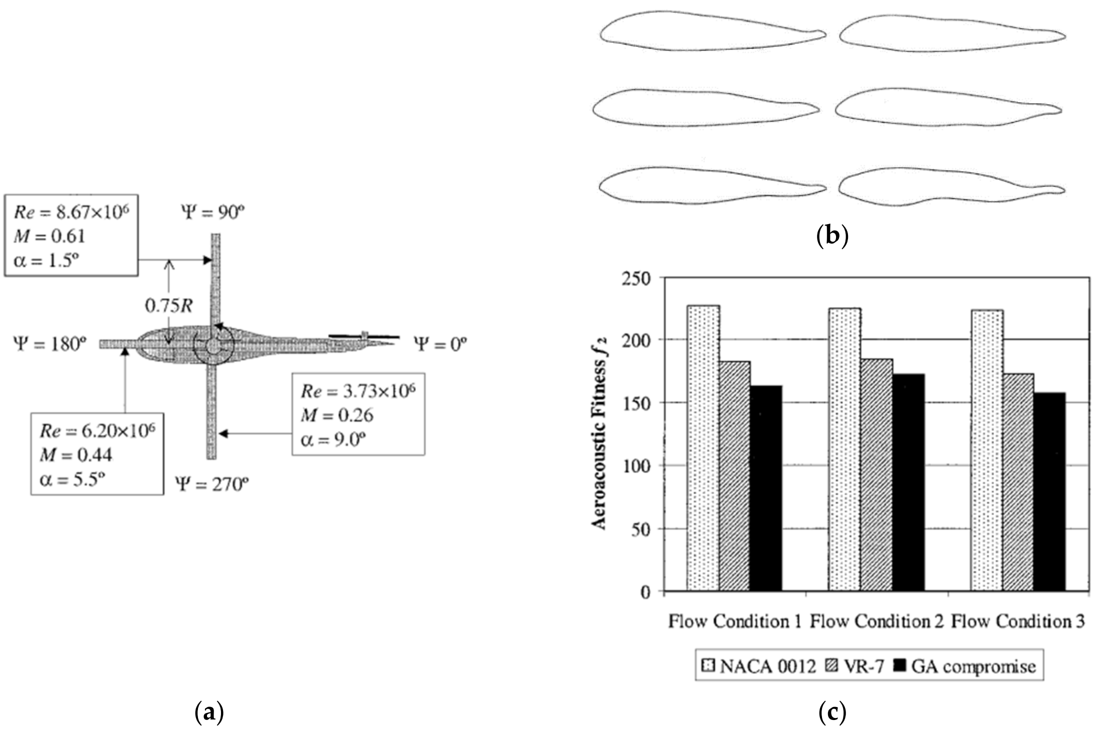

Figure 7. (**a**). Airfoil Design Conditions; (**b**). Resulting optimal airfoil shapes; (**c**). Plots showing Aeroacoustic fitness benefits [34]. Reprinted with permission from Lyrintzis, A.S. (2010).

4. Active Noise Control (ANC) Technology

Reducing noise radiation via passive control may have adverse effects on the aerodynamic performance. Therefore, an alternative approach is to design the vehicle with some passive control built-in the design, which should be optimized for regular flight operations then engage ANC only in particular situations when the noise temporarily increases above the allowable level as in the vicinity of vertiport.

The notional principle that the sound pressure can be mitigated by superimposing a secondary noise source that is in phase with but opposite in amplitude to the primary source was first introduced by Lueg [38]. Lueg's idea developed eventually into the field of active noise control. Three main classifications of active noise control mechanisms were devised—Zone Control, On-blade or source modification, and sound absorption [39]. For simplicity, the sound absorption mechanism would be omitted as it pertains mainly to the fuselage/cabin noise control.

4.1. Zone Control

The first type of ANC is sound field cancellation or zone control. To execute a zone control, a zone of silence is needed around the sound source. One method for achieving this is the use of anti-noise. The basic principle is that if the noise at the target point is a simple wave, one can impose an identical wave to it with a 180 degrees phase shift to cancel it. An example of this mechanism is the noise cancelling headphones, first developed by Meeker of RCA [40]. Practical applications of this kind of mechanism are limited to relatively enclosed regions. Usually, a feedback loop is needed. A sensor measures the radiated sound, which is fed into a microprocessor to determine the anti-noise signal needed for sound suppression. Complete cancellation at a given point, in principle, can be achieve via an iterative process through the feedback mechanism. Ikelheimer & Nagel [41] considered a propeller surrounded by four speakers to create a zone of silence. The method worked best at the specific target location, but other locations saw increases in the sound pressure level. Increasing the number of speakers was found to be more effective. Deviating slightly from rotors, some successes have been seen in experiments by Koopmann et al. [42] with

10–20 dB noise reductions in centrifugal fans. This technique becomes unfeasible for open rotors as it would require a high acoustic impedance to counter the noise source for every observer location [41].

4.2. On-Blade Actuation

The second type of ANC is the modification or suppression of the sound generation, is the case where a modification is done on the blade to alter the radiation impedance of the original noise source for acoustic mitigation. Most active rotor noise control ideas fall under this mechanism or classification. Several decades of research and studies were directed towards BVI noise reduction, vibration reduction, and performance enhancement [43–45]. On-blade active rotor control methods such as higher harmonic control (HHC), individual blade control (IBC), trailing edge flap (TEF), blowing on or near the rotor blade have been tested as potential ways of altering the wake structure, and subsequently the reduction of the BVI effects [44].

Higher harmonic control system is an active vibration control mechanism where the rotor blades are oscillated at higher harmonics of the rotational speed. Although originally devised as a method for vibrational reduction, it was suggested as a potential method for reducing BVI in the late 1990s [45]. However, it was determined that when implemented, fuselage vibration levels were drastically increased when driven at low BVI noise frequencies [46,47]. This can be reduced by applying the excitation at a higher harmonic frequency, which ultimately led to the development of the individual blade control methods. eVTOLs are generally scaled down variants of rotorcrafts with multiple rotor systems. Applying this method of active rotor control might prove quite deleterious as the vibrations or excitation of the oscillations from all the rotors might introduce some structural issues and may reduce the level of comfort in the fuselage/cabin. Several active control research have been done particularly for helicopter rotors with little to none done for small-scale rotors for UAVs. However, we review a few techniques and their feasibility and successes.

Anobile et al. [48] developed a low-frequency controller geared towards reducing helicopter rotor BVI noise. The utilize an active twist rotor concept via torque load distributions at 2/rev frequency. They apply this methodology numerically to a scaled Bo-105 4-bladed helicopter main rotor, with a radius of 2 m, a constant chord of 0.212 m, linear twist of -8 degrees, and a rotational speed of 109 rad/s. The general Kussner-Schwarz theory is employed to determine the unsteady aerodynamic loads associated with the profile downwash. Aeroelastic computations are performed to account for the blade deformation and its effects on the wake. The wake inflow is predicted using a free-wake boundary element solver. They perform open-loop control using the active twist, which showed that a 2/rev actuation was effective in reducing the BVI sound pressure level by about 2 dB. However, this also resulted in an increase in vibratory loads and low frequency noise of about 3 dB. Using the microphones below helicopter and at the skid ends (Figure 8a), a closed loop controller was developed which resulted in a maximum BVI sound pressure level reduction of 6 dB at the retreating side.

One of the earliest proven tests of the concept of on-blade actuation for harmonic noise control was the full-scale “Boeing SMART” rotor [49]. They utilized an active trailing edge flap for the blade noise control. The results showed that placing the controls near the tips is an effective thickness noise control, with the total thickness noise reduced to about 50% in amplitude.

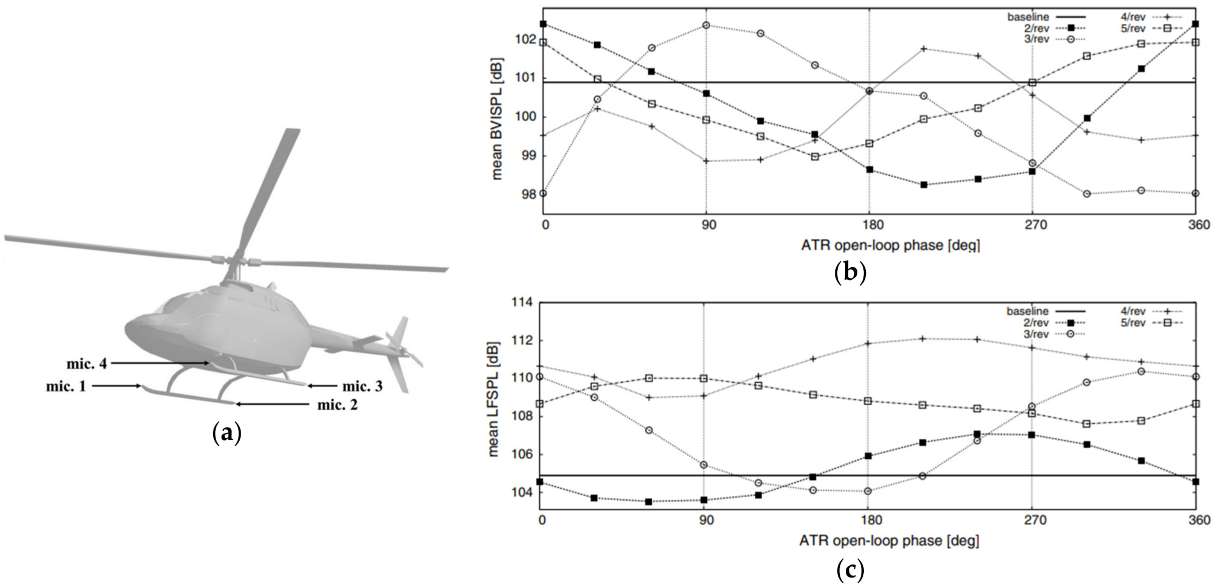

Figure 8. (**a**). Location of microphones; (**b**). Mean BVI sound pressure level for open-loop controller; (**c**). Mean Low-frequency Sound Pressure Level [48]. Reprinted with permission from Anobile, A. (2016).

More recently, Sargent and Schmitz [43,50,51] performed experiments with a 1/7th scale rotor, where they used tip mass ejection to attempt to reduce specifically the in-plane thickness noise. They implement this by extracting out the mass flow rate equation and comparing with the Ffowcs-Williams Hawking equation (Ffowcs Williams and Hawkings, 1969). For an idealized point source ejecting mass into a quiescent medium, the jet mass flow rate is given as [51]:

$$\dot{m}_{jet} = \rho_{jet} A_{jet} V_{jet} \tag{1}$$

With velocity of source moving with respect to the medium $\vec{V}_{source} = \vec{\Omega}\ x\ \vec{r}_{jet} + \vec{V}_\infty$. Assuming $\rho_{jet} = \rho_0$ then:

$$\vec{F}_{jet} = \dot{m}_{jet}\left(\vec{V}_{jet} + \vec{V}_{source}\right) = \dot{m}_{jet}\left(\vec{V}_{jet} + \vec{\Omega}\ x\ \vec{r}_{jet} + \vec{V}_\infty\right) \tag{2}$$

Comparing with FWH equation, we get the permeable mass and momentum injection terms as:

$$Q = \rho A(u_n - v_n) \text{ and } \vec{F} = \rho A \vec{u}(u_n - v_n) \tag{3}$$

where $\vec{u} = \vec{V}_{jet} + \vec{V}_{source}$ and $\vec{v} = \vec{V}_{source}$. The anti-noise acoustic pressure was derived to be the combination of the pressure due to the mass injection term, and that due to the momentum injection. This method resulted in a reduction in the peak negative amplitude of the test rotor's radiated noise by 5 Pa at the target microphone, but was impractical as the required mass flow rate needed required a high exit jet velocity profile (see Figure 9).

Shi et al. [52] explored the use of trailing edge winglets for unsteady force excitation. This method specifically looks to target the rotor thickness noise. The method involves the application of an unsteady aerodynamic force to excite a secondary or anti-sound wave. This excitation was done with the use of a trailing edge winglet near the tip of the rotor (see Figure 10).

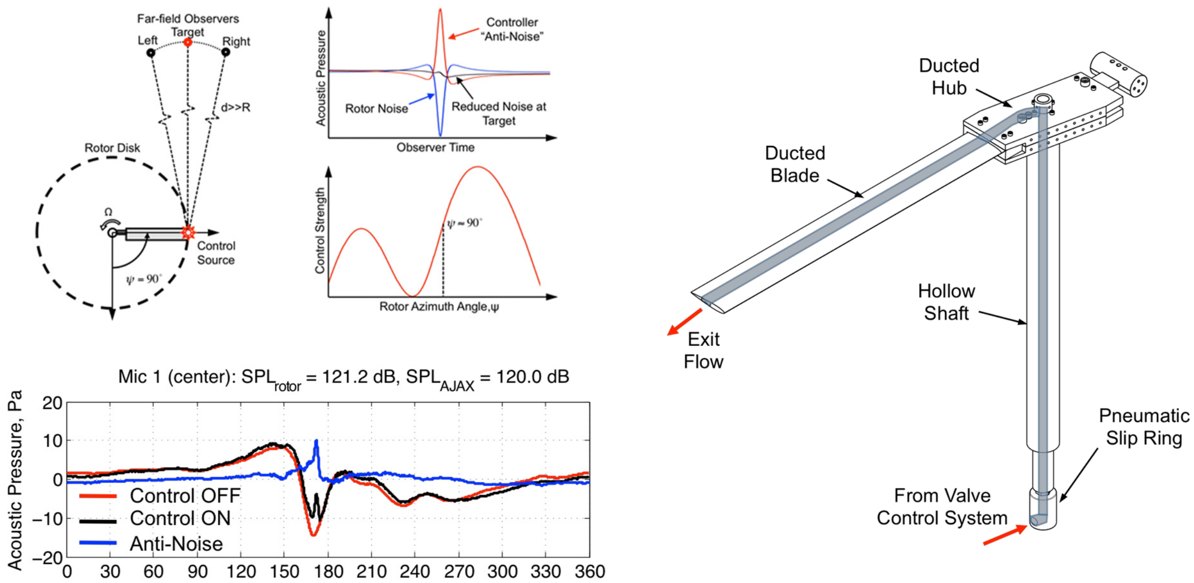

Figure 9. Experimental Setup for tip air blowing [50]. Reprinted with permission from Sargent, D.C. (2014).

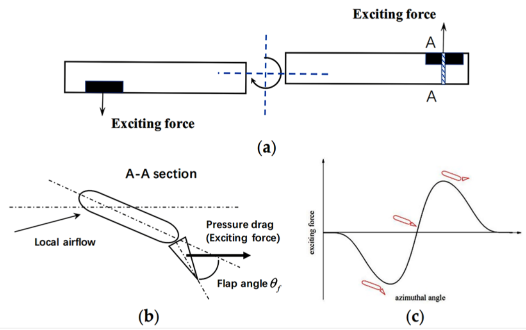

Figure 10. Schematic of experimental setup [52].

A harmonic formulation for prescribing the motion of the trailing edge winglet actuator was devised:

$$F = F_n \sin(n\psi + \psi_o) \tag{4}$$

where F_n is amplitude, n is the harmonic, ψ and ψ_o are azimuthal angle and initial excitation angle. The limitations of this approach are that the formulation of the anti-noise actuation depends on the correct amplitude of the forcing function, F_n, the harmonic number, and the phase angle (see Figure 11). There was no direct correlation to obtain the exact wave form without experimentation.

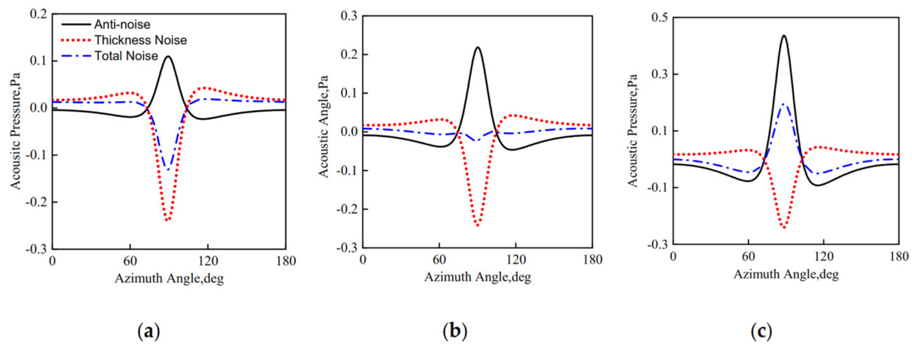

Figure 11. Effect of force amplitude on noise reduction. (**a**) F_n = 2 N, (**b**) F_n = 4 N, (**c**) F_n = 8 N [52].

Another approach was devised by Yang et al. [53] by canceling the in-plane thickness noise with a point source loading noise formulation. They utilize a single-bladed rotor with a radius of 5.79 m, a chord of 0.381 m, and an advancing-tip Mach number of $M_{AT} = 0.8$ with a target observer 100 Radii away from the center of the rotor. From the differential form of the FWH equation, the loading noise is formulated by equating the thickness noise at an observer to the loading noise:

$$p'_L(x,t) = -p'_T(x,t) \quad (5)$$

This technique was implemented both numerically and experimentally using a flap for a single observer and a single rotor blade.

They tested two actuators—an active flap and a winglet on the blades and found that the active flap resulted in about 3 dB noise reduction over an azimuth range of 150 to 210 degrees, and the winglet showed more than 6 dB reduction over an azimuthal range of 120 to 240 degrees in the rotor plane.

All the discussed methods have proven to be successful in cancelling thickness noise, but the practicality of the applications is still questionable. The use of the active flaps showed great promise, but its effects on the blade loading and performance, as well as the structural integrity of the blades is yet to be understood. Additionally, the methods discussed have all been tested on single rotor blades, and thus their applicability in multi-bladed and multi-rotor systems must be explored.

4.3. Active Tonal Noise Control of Multi-Rotor Air Mobility Vehicles at Approach

ANC of rotors has been investigated recently by [54], Yang et al. (2019). [50], and [49], among others. They argued that it is the in-plane fundamental thickness noise that needs to be reduced as it becomes the significant source during approach. This is particularly true with the low-frequency high amplitude noise. They proposed placing a point actuator on the blades to produce some loading noise to cancel the in-plane thickness noise. Actuators such as a flap, winglets and tip-blowing have been investigated. The above-mentioned work is, however, limited to the case of a single rotor, and a single actuator. Single point actuators make the loading actuation per area too excessive. Extension to AAM multi-rotors with distributed actuators is needed and is the subject of Afari & Mankbadi's [55] work.

An Active Noise Control (ANC) technology is developed by Afari & Mankbadi [55] to reduce the in-plane thickness noise associated with multi-rotor Advanced Air Mobility Vehicles (AAM). They considered two in-line rotors and showed that the FWH-determined actuation signal can produce perfect cancellation at a point target. However, the practical need is to achieve noise reduction over an azimuthal zone, not just a single point. Furthermore, for practical applications the single point actuator is replaced by distributed micro actuators system (Figure 12). Note that F_s is the span-wise force, F_c is the chord-wise force, and L_r is the resultant loading vector in the target observer direction. To achieve this zonal noise reduction, an optimization technique is developed to determine the required actuation signal produced by the on-blade distribution of embedded actuators on the two rotors.

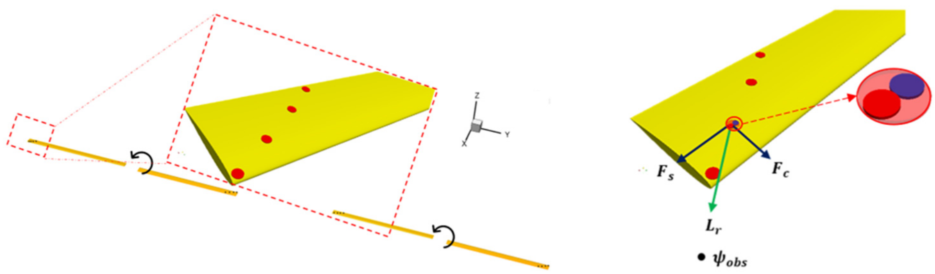

Figure 12. Sketch showing the directivity of the forces and the loads in relation to the observer as well as the dual piezo speaker configuration [55].

4.4. Calculation of Distributed Array of Loading Actuators

A distributed array of acoustic actuators is used for imposing the required loading noise needed to reduce the noise at a set of azimuthal observers. From the Farassat's formulation 1A [56], the total acoustic pressure at an observer point is given as:

$$p'(x,t) = p'_T(x,t) + p'_L(x,t), \tag{6}$$

To find the loading solution, we set $p'_L(x,t) = -p'_T(x,t)$. If we assume the blade surface to be a compact source, the loading noise formulation becomes:

$$p'_{L_{Anti}}(x,t) = \frac{1}{4\pi c_0} \sum_{i=1}^{nB*nR} \left[\frac{1}{r_i(1-M_{r_i})^2} \frac{\partial L_{r_i}}{\partial \tau} + \frac{c_0 L_{r_i}}{r_i^2(1-M_{r_i})} + \frac{L_{r_i}\left(r_i \dot{M_{ri}} + c_0 M_{r_i} - c_0 M^2\right)}{r^2(1-M_{r_i})^3} \right]_{ret} \tag{7}$$

where L_r is the component of the loading solution in the radiation direction, nB and nR are the number of blades and number of rotors, respectively. The anti-noise loading L_r needed is then solved by feeding the values of the thickness noise, p'_T, and getting values of the observer distance r, the Mach number in the radiation direction M_r, and the flight Mach number M from the computation of the thickness noise into the ordinary differential equation shown in Equations (8) and (9). A fourth order Runge-Kutta algorithm is employed to solve for the loading "anti-noise" solution, which is then fed into Equation (7) to find the corresponding anti-noise pressure signal.

$$\frac{dL_r}{d\tau} + p(\tau)L_r = r(\tau) \tag{8}$$

where

$$p(\tau) = \sum_{i=1}^{nB*nR} \left[\frac{c_0(1-M_{r_i})^2 + r_i \dot{M}_{r_i} + c_0\left(M_{r_i} - M^2\right)}{r_i(1-M_{r_i})} \right] \tag{9}$$

$$r(\tau) = -4\pi c_0 \frac{p'_T}{\varepsilon} \sum_{i=1}^{nB*nR} r_i(1-M_{r_i})^2 \tag{10}$$

Target Zone: For a zone of target observers, a new loading term, L_{rA}, is introduced such that:

$$L_{rA,i} = \sum_{j=1}^{nObs*nR*nB} B_j K_j L_{r,j} \tag{11}$$

where K_j and B_j are the coefficients and tuning parameters that needs to be solved. This function is looped over each blade and each rotor, and thus the number of tuning parameters increase. The resulting optimized loading solution, L_r as well as far-field noise signal are shown in Figure 13. The far-field pressure field is also computed and shown in Figure 14. We see a slightly imperfect total cancellation. This occurs because the loading actuator must account for each observer peak, which is offset, and is not at the same temporal location. For the specific geometry, this produced about 9 dB reduction in the in-plane thickness noise during forward flight of the two rotors. Note that although the method works well for thickness noise control, broadband noise might prove to be important for AAM, and thus the method would need to be extended for BBN control.

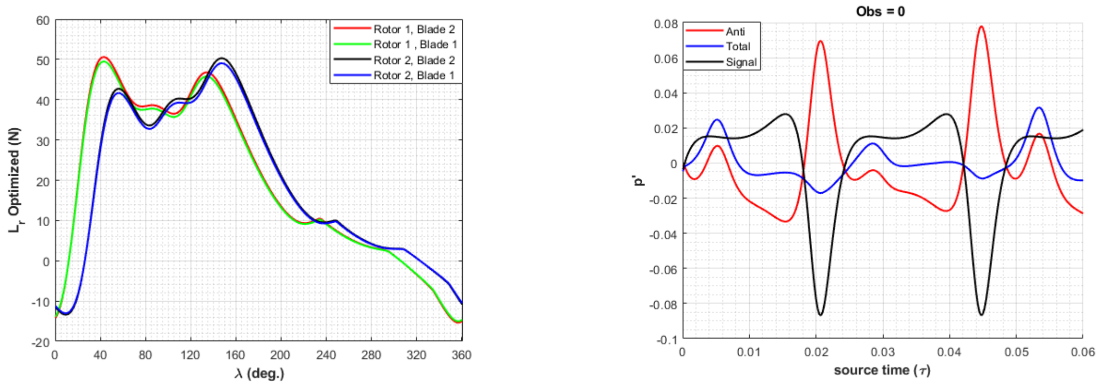

(**a**) (**b**)

Figure 13. (**a**) Optimized Loading Solution, L_r, for each blade; (**b**) Total Noise at target observer, $\psi_{obs} = 0^{o}$.

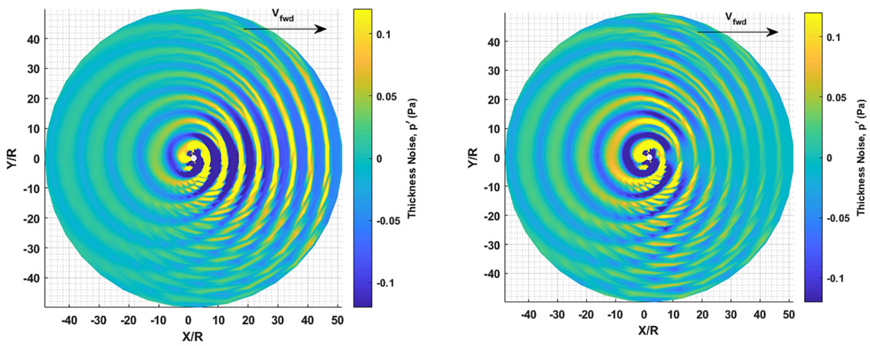

(**a**) (**b**)

Figure 14. Contour plots of acoustic pressure showing (**a**): No control, and (**b**): With control for a zone of observers [55].

5. Discussion

Several passive control methods are reviewed, from leading edge trip, trailing edge serrations, leading edge notch, effects of blade counts, and ducts. These methods showed some successes in mitigating the noise of the blades, but ultimately affects the performance of the rotors. Several works tackled this problem by optimizing the design process with performance constraints [32,34]. These still have some trade-offs that may work as intended but may result in difficulty in manufacturing or may present some structural difficulties.

To overcome the physical modifications, we looked at several active control methods. Zone cancellation was found to be infeasible for open rotors as it would require a high acoustic impedance to counter the noise source for every observer location [41]. For on-blade source manipulations, taking some notes from several decades of active BVI noise control in legacy helicopters, the active twist methodology [48] showed improvements in the overall noise reduction in the higher frequencies, but were detrimental at the lower frequencies. Perhaps this approach can be applied to specific stages of the flight envelope, for example, during approach/landing phase, where blade-wake interactions are highest. The pulsed tip jets method [43] showed some acoustic benefits but required cumbersome jet configurations and equipment, which imposes a weight penalty on the vehicle. The winglets and trailing edge flaps also showed good acoustic benefits but may add a structural penalty to the rotor blades. As a possible remedy, an on-blade actuation using an embedded speaker system may require less structural loads and weight. The techniques discussed have been applied to single rotor blades, thus there is a need to investigate their effectiveness in multi-bladed and multi-rotor applications as in the case of Afari & Mankbadi [55] Additionally, there is a need for a high-fidelity analysis of the above methods and their effectiveness in more realistic conditions.

Overall, a great deal of research has been performed on understanding propeller and rotor noise sources, as well as predicting them accurately. Research on the control of these noise sources has been ongoing, but with allusions to helicopter rotors, they show great promise for total noise control with the eventual hope to apply the methods to the emergence of urban air mobility vehicles.

Closed Loop ANC: The actual radiated sound is expected to differ from that obtained by the simplified methodologies discussed above. Therefore, a feedback loop is needed to measure/estimate the radiated sound and decide on adjusting the actuator signal accordingly. Similar work is done by Anobile et al. [48], but targets the rotor floor or region below the rotor. This may be useful, again during descent or highly impulsive vehicles (helicopters). For typical AAM vehicles, the BVI phenomena is not as pronounced and thus the in-plane thickness noise may be more prominent especially on approach. With this, we cannot apply this method of feedback control. We can measure some of the near-field parameters, such as the fluctuating pressure, as a surrogate parameter for the far field noise. However, to develop a closed-loop controller, a Reduced-Order Model (ROM) may be useful.

Anti-Noise and Machine learning (ML): When applying the anti-noise principle to AAM it becomes too complicated. First, because the radiated signal is composed of tonal and broadband noise over a range of frequencies, and secondly, because we want to cancel or reduce the noise in more than one point. Sensing and analyzing the radiated sound and determining the proper anti-noise signal is difficult in real time and for multi-observer points, which makes anti-noise a challenge for AAM (e.g., Ikelheimer & Nagel [41], Stevens & Ahuja [57].

If ML can be used to provide a relatively quick analysis of multiple points of the radiated noise, and provide the anti-noise signal, then speakers mounted on the AAM can possibly generate the needed signal relatively instantaneously. High-fidelity simulations can be used develop a Reduce-Order Model (ROM), then use this ROM to train the ML model to predict in real time the radiated noise and its anti-noise optimized signal for a zone of silence.

Author Contributions: Conceptualization, R.M. and S.A.; methodology, S.A.; writing—original draft preparation, S.A.; writing—review, supervision, and editing, V.G., A.S.L. and R.M. All authors have read and agreed to the published version of the manuscript.

Funding: This research received no external funding.

Institutional Review Board Statement: Not applicable.

Informed Consent Statement: Not applicable.

Data Availability Statement: No new data were created.

Acknowledgments: Golubev acknowledges partial support for the publication preparation in the implementation of the program for the creation and development of the World-Class Research Center "Supersonic" for 2020–2025 funded by the Ministry of Science and Higher Education of the Russian Federation (Grant agreement of 17 May 2022 No. 075-15-2022-1023), and partial support from PRUE university.

Conflicts of Interest: The authors declare no conflict of interest.

References

1. Runway Safety | Federal Aviation Administration. Available online: https://www.faa.gov/newsroom/runway-safety-0 (accessed on 19 May 2022).
2. Brookhouser, P.E. Prevention of Noise-Induced Hearing Loss. *Prev. Med.* **1994**, 23. [CrossRef] [PubMed]
3. Franssen, E.; van Wiechen, C.; Nagerlkerke, N.; Lebret, E. Aircraft noise around a large international airport and its impact on general health and medication use. *Occup. Environ. Med.* **2004**, *61*, 405–413. [CrossRef] [PubMed]
4. Haines, M.; Stansfeld, S.A.; Job, R.; Berglund, B.; Head, J. Chronic aircraft noise exposure, stress responses, mental health, and cognitive performance in school children. *Psychol. Med.* **2001**, *31*, 265–277. [CrossRef] [PubMed]

5. Stansfeld, S.; Berglund, B.; Clark, C.; Lopez-Barrio, I.; Fischer, P.; Öhrström, E.; Haines, M.; Head, J.; Hygge, S.; van Kamp, I.; et al. Aircraft and road traffic noise and children's cognition and health: A cross-national study. *Lancet* **2005**, *365*, 1942–1949. [CrossRef]
6. Hubbard, H.H. *Aeroacoustics of Flight Vehicles: Theory and Practice Volume 1: Noise Sources*; NASA: Greenbelt, MD, USA, 1991.
7. Lu, Z.; Debiasi, M.; Khoo, C. Acoustic characteristics of a multi-rotor MAV and its noise reduction technology. In *INTER-NOISE and NOISE-CON*; Ingenta Connect: New Brunswick, NJ, USA, 2016; pp. 393–403. Available online: http://www.ingentaconnect.com/content/ince/incecp/2016/00000253/00000008/art00043#expand/collapse (accessed on 20 August 2020).
8. Bellocq, P.; Garmendia, I.; Sethi, V.; Patin, A.; Capodanno, S.; Rodriguez Lucas, F. Multidisciplinary Assessment of the Control of the Propellers of a Pusher Geared Open Rotor-Part I: Zero-Dimensional Performance Model for Counter-Rotating Propellers. *J. Eng. Gas Turbine Power* **2016**, 138. [CrossRef]
9. Tang, Z.; Liu, P.; Chen, Y.; Guo, H. Experimental Study of Counter-Rotating Propellers for High-Altitude Airships. *J. Propuls. Power* **2015**, *38*, 1491–1496. [CrossRef]
10. Diaz, P.V.; Rubio, R.C.; Yoon, S. Simulations of ducted and coaxial rotors for air taxi operations. In Proceedings of the AIAA Aviation 2019 Forum, Dallas, TX, USA, 17–21 June 2019. [CrossRef]
11. Stoll, A. *Design of Quiet UAV Propellers*; Stanford University: Stanford, CA, USA, 2012.
12. Pascioni, K.A.; Rizzi, S.A.; Schiller, N.H. Noise reduction potential of phase control for distributed propulsion vehicles. *AIAA Scitech 2019 Forum.* **2019**. [CrossRef]
13. Grosveld, F. Calibration of the structural acoustics loads and transmission facility at NASA Langley Research Center. *Proc. Inter-Noise* **1999**, *99*, 1541–1546.
14. Smith, B.; Gandhi, F.; Chair, R.; Niemiec, R. A Comparison of Multicopter Noise Characteristics with Increasing Number of Rotors. In Proceedings of the Vertical Flight Society's 76th Annual Forum, Virtually, 5–8 October 2020.
15. Whiteside, S.; Zawodny, N.; Fei, X.; Pettingill, N.A.; Patterson, M.D.; Rothhaar, P. An Exploration of the Performance and Acoustic Characteristics of UAV-Scale Stacked Rotor Configurations. In Proceedings of the AIAA SciTech 2019 Forum, San Diego, CA, USA, 7–11 January 2019. [CrossRef]
16. Leslie, A.; Wong, K.C.; Auld, D. Broadband noise reduction on a mini-UAV propeller. In Proceedings of the 14th AIAA/CEAS Aeroacoustics Conference (29th AIAA Aeroacoustics Conference), Vancouver, BC, Canada, 5–7 May 2008. [CrossRef]
17. Cambray, A.; Pang, E.; Showkat Ali, S.A.; Rezgui, D.; Azarpeyvand, M. Investigation towards a better understanding of noise generation from UAV propellers. In Proceedings of the 2018 AIAA/CEAS Aeroacoustics Conference, Atlanta, Georgia, 25–29 June 2018. [CrossRef]
18. Intravartolo, N.; Sorrells, T.; Ashkharian, N.; Kim, R. Attenuation of vortex noise generated by UAV propellers at low Reynolds numbers. In Proceedings of the AIAA SciTech Forum—55th AIAA Aerospace Sciences Meeting, Grapevine, TX, USA, 9–13 January 2017. [CrossRef]
19. Nelson, T.J. *Practical Modifications for Low Reynolds Number Propeller Applications*; Wichita State University: Wichita, KS, USA, 2005.
20. Demoret, A.C.; Wisniewski, C.F. The impact of a notched leading edge on performance and noise signature of unmanned aerial vehicle propellers. In Proceedings of the AIAA Scitech 2019 Forum, San Diego, CA, USA, 7–11 January 2019. [CrossRef]
21. Schmitz, F.H. The challenges and possibilities of a truly quiet helicopter: 29th Alexander A. Nikolsky honorary lecture. *J. Am. Helicopter Soc.* **2016**, *61*, 041001-1–041001-33. [CrossRef]
22. Martins, J.R.R.A. *A Short Course on Multidisciplinary Design Optimization (Vol. 18)*; University of New South Wales Australia: Sydney, Australia, 2012.
23. Pironneau, O. On optimum design in fluid mechanics. *J. Fluid Mech.* **1974**, *64*, 97–110. [CrossRef]
24. Haftka, R.T. Optimization of flexible wing structures subject to strength and induced drag constraints. *AIAA J. Aircr.* **2012**, *15*, 1101–1106. [CrossRef]
25. Grossman, B.; Gurdal, Z.; Haftka, R.T.; Strauch, G.J.; Eppard, W.M. Integrated Aerodynamic/Structural Design of a Sailplane Wing. *AIAA J. Aircr.* **2012**, *25*, 855–860. [CrossRef]
26. Manning, V.M. *Large-Scale Design of Supersonic Aircraft via Collaborative Optimization*; Stanford University: Stanford, CA, USA, 1999. Available online: https://ui.adsabs.harvard.edu/abs/1999PhDT.......284M/abstract (accessed on 21 May 2022).
27. Kroo, I.; Altus, S.; Braun, R.; Gage, P.; Sobieski, I. Multidisciplinary optimization methods for aircraft preliminary design. In Proceedings of the 5th Symposium on Multidisciplinary Analysis and Optimization, Panama City Beach, FL, USA, 7–9 September 1994; pp. 697–707. [CrossRef]
28. Ganguli, R. A Survey of Recent Developments in Rotorcraft Design Optimization. *AIAA J. Aircr.* **2012**, *41*, 493–510. [CrossRef]
29. Glaz, B.; Friedmann, P.P.; Liu, L. Helicopter Vibration Reduction throughout the Entire Flight Envelope Using Surrogate-Based Optimization. *J. Am. Helicopter Soc.* **2009**, 54. [CrossRef]
30. Amiet, R.K. Noise Due to Turbulent Flow Past a Trailing Edge. *J. Sound. Vib.* **1976**, *47*, 387–393. [CrossRef]
31. Pagano, A.; Barbarino, M.; Casalino, D.; Federico, L. Tonal and broadband noise calculations for aeroacoustic optimization of propeller blades in a pusher configuration. *AIAA J. Aircr.* **2010**, *43*, 3. [CrossRef]
32. Marinus, B.G.; Roger, M.; van den Braembussche, R.A.; Bosschaerts, W. Multidisciplinary optimization of propeller blades: Focus on the aeroacoustic results. In Proceedings of the 17th AIAA/CEAS Aeroacoustics Conference 2011 (32nd AIAA Aeroacoustics Conference), Portland, OR, USA, 5–8 June 2011. [CrossRef]
33. Ffowcs Williams, J.E.; Hawkings, D.L. Sound generation by turbulence and surfaces in arbitrary motion. *Philos. Trans. R. Soc. London. Ser. A Math. Phys. Sci.* **1969**, 264. [CrossRef]

34. Jones, B.R.; Crossley, W.A.; Lyrintzis, A.S. Aerodynamic and Aeroacoustic Optimization of Rotorcraft Airfoils via a Parallel Genetic Algorithm. *AIAA J. Aircr.* **2010**, *37*, 1088–1096. [CrossRef]
35. Drela, M. XFOIL: An Analysis and Design System for Low Reynolds Number Airfoils. *Low Reynolds Number Aerodyn.* **1989**, *54*, 1–12. [CrossRef]
36. Brentner, K.S. *Prediction of Helicopter Rotor Discrete Frequency Noise: A Computer Program Incorporating Realistic Blade Motions and Advanced Acoustic Formulation*; NASA Technical Memorandum 87721; NASA: Greenbelt, MD, USA, 1986.
37. Ingraham, D.; Gray, J.; Lopes, L.V. Gradient-based propeller optimization with acoustic constraints. In Proceedings of the AIAA SciTech 2019 Forum, San Diego, CA, USA, 7–11 January 2019. [CrossRef]
38. Lueg, P. Process of Silencing Sound Oscillations. U.S. Patent Application No. 2043416, 9 June 1936.
39. Bies, D.A.; Hansen, C.H. *Engineering Noise Control*, 2nd ed.; Bies, D.A., Hansen, C.H., Eds.; CRC Press: Boca Raton, FL, USA, 2017. [CrossRef]
40. Cunefare, K. *Active Noise Control. Special Lay-Language Paper for the 75th Anniversary Meeting of the Acoustical Society of America*; ASA: Melville, NY, USA, 2004.
41. Ikelheimert, B.J.; Nagel, R.T. Active noise control of an unducted model propeller. In Proceedings of the 3rd AIAA/CEAS Aeroacoustics Conference, Atlanta, GA, USA, 12–14 May 1997; pp. 441–447. [CrossRef]
42. Koopmann, G.H.; Koopmann, W.; Chen, W. Active Noise Control to Reduce the Blade Tone Noise of Centrifugal Fans. *J. Vib. Acoust. Stress Reliab. Des.* **1988**, *110*, 377–383. [CrossRef]
43. Sargent, D.C. *Active Jet Acoustic Control of Low Frequency, In-Plane Helicopter Harmonic Noise*; University of Maryland: College Park, MD, USA, 2012.
44. Yu, Y.H.; Gmelin, B.; Splettstoesser, W.; Philippe, J.J.; Prieur, J.; Brooks, T.F. Reduction of helicopter blade-vortex interaction noise by active rotor control technology. *Prog. Aerosp. Sci.* **1997**, *33*, 647–687. [CrossRef]
45. Hardin, J.C.; Lamkin, S.L. Concepts for reduction of blade/vortex interaction noise. *AIAA J. Aircr.* **2012**, *24*, 120–125. [CrossRef]
46. Brooks, T.F.; Booth, E.R.; Jolly, J.J.R.; William, J.R.; Yeager, T.; Matthew, J.R.; Wilbur, L. *Reduction of Blade-Vortex Interaction Noise through Higher Harmonic Pitch Control*; American Helicopter Society: Phoenix, AZ, USA, 1990; Volume 35.
47. Splettstoesser, W.R.; Lehmann, G.; van der Wall, B. Higher harmonic control of a helicopter rotor to reduce blade-vortex interaction noise. *Z. Fluowissenschaften* **1996**, *14*, 109–116.
48. Anobile, A.; Bernardini, G.; Gennaretti, M.; Testa, C. Synthesis of Active Twist Controller for Rotor Blade–Vortex Interaction Noise Alleviation. *J. Aircr.* **2016**, *53*, 1865–1874. [CrossRef]
49. Sim, B.W.; JanakiRam, R.D.; Lau, B.H. Reduced in-plane, low-frequency noise of an active flap rotor. *J. Am. Helicopter Soc.* **2014**, *59*, 1–17. [CrossRef]
50. Sargent, D.C.; Schmitz, F.H. Fundamental experimental studies supporting active-jet acoustic control of in-plane rotor harmonic noise. *J. Aircr.* **2014**, *51*, 434–446. [CrossRef]
51. Caleb Sargent, D.; Schmitz, F.H. Fundamental experimental studies supporting on-blade tip air blowing control of in-plane rotor harmonic noise. In Proceedings of the 18th AIAA/CEAS Aeroacoustics Conference (33rd AIAA Aeroacoustics Conference), Colorado Springs, CO, USA, 4–6 June 2012. [CrossRef]
52. Shi, Y.; Li, T.; He, X.; Dong, L.; Xu, G. Helicopter Rotor Thickness Noise Control Using Unsteady Force Excitation. *Appl. Sci.* **2019**, *9*, 1351. [CrossRef]
53. Yang, T.; Brentner, K.S.; Corle, E.; Schmitz, S. Study of active rotor control for in-plane rotor noise reduction. *J. Aircr.* **2019**, *56*, 179–190. [CrossRef]
54. Gopalan, G.; Schmitz, F. Far-Field Near-In-Plane Harmonic Main Rotor Helicopter Impulsive Noise Reduction Possibilities. *Am. Helicopter Soc. Annu. Forum* **2008**, *64*, 675.
55. Afari, S.O.; Mankbadi, R.R. Active Noise Control of Multi-Rotor Advanced Air Mobility Vehicles. *J. Am. Helicopter Soc.* **2022**, 63. [CrossRef]
56. Brentner, K.S. Modeling aerodynamically generated sound: Recent advances in rotor noise prediction. In Proceedings of the 38th Aerospace Sciences Meeting and Exhibit, Reno, NV, USA, 10–13 January 2000. [CrossRef]
57. Stevens, J.C.; Ahuja, K.K. Recent advances in active noise control. *AIAA J.* **1991**, *29*, 1058–1067. [CrossRef]